Sedimentation of Oblate Ellipsoids at low and Moderate Reynolds numbers

F. Fonseca and H. J. Herrmann

ICA-1, University of Stuttgart, Pfaffenwaldring 27, 70569 Stuttgart, Germany

Abstract

In many applications to biophysics and environmental engineering, sedimentation of non-spherical particles for example: ellipsoids, is an important problem. In our work, we simulate the dynamics of oblate ellipsoids under gravity. We study the settling velocity and the average orientation of the ellipsoids as a function of volume fraction. We see that the settling velocity shows a local maximum at the intermmediate densities unlike the spheres. The average orientation of the ellipsoids also shows a similar local maximum and we observe that this local maximum disappears as the Reynolds number is increased. Also, at small volume fractions, we observe that the oblate ellipsoids exhibit an orientational clustering effect in alignment with gravity accompanied by strong density fluctuations. The vertical and horizontal fluctuations of the oblate ellipsoids are small compared to that of the spheres.

Key words:

1 Introduction

The sedimentation of particles in a fluid under the action of gravity is an interesting problem in fluid dynamics and statistical physics which finds application in biology, environmental and industrial engineering. For example, chemical reactors, pollution, ink-jet printing, blood, fluidized beds, etc. This problem reveals complicated multi-body interactions due to the long-range hydrodynamics, that decay for a sphere as $1/r$, where r is the distance between the particles. The particle velocities strongly fluctuate and there has been some controversy about the nature of these velocity fluctuations, [1].

In the dilute case and low Reynolds numbers, the behavior of the settling velocity $V(\phi)$ as a function of the volume fraction Φ, in the limit where Brownian motion is negligible, has been investigated by Batchelor[2]. $V(\Phi)$ decreases

monotonically as Φ increases following the phenomenological Richardson-Zaki law [3].

Much of the investigations have been made on the spheres and in a reduced manner on slender bodies, e.g. fibers by [1,4]. Fibers have many technological applications[7]. An orientational transition is well known for smaller volumer fractions, which is characterized by a maximum in the sedimentation velocity [8]. Ellipsoidal particles find applications in the models for blood flow [5], car paint and sun protectors.

In our previous work [15], we have constructed a phase-diagram where three basic regimes exist namely steady-falling, oscillatory and chaotic regime for a single oblate. In this paper, we present results of the simulation of many oblates sedimenting in the fluid under gravity, in the steady falling regime of a single oblate. The rest of the paper is organized as follows. In section 2, we discuss the model, in section 3.1, we present the behavior of sedimentation velocity, in 3.2, we discuss the orientation of ellipsoids, in 3.3, we discuss orientational order parameter. In section 3.4, we present results at moderate Reynolds number with not very large aspect ratios followed by summary and conclusion in section 4.

2   Model

The model was developed by Höefler and Schwarzer [10,11], extended by Kuusela et al [12] and has been applied to several studies [14,15]. The fluid motion is solved by discretizing on a mesh [11], the incompressible Navier-Stokes equations:

$$\frac{\partial \vec{v}}{\partial t} + (\vec{v} \cdot \vec{\nabla})\vec{v} = -\vec{\nabla}p + \frac{1}{Re}\nabla^2\vec{v} + \vec{f}$$
$$\vec{\nabla} \cdot \vec{v} = 0 \tag{1}$$

where $\vec{v}$ is the fluid velocity, p the pressure and $\vec{f}$ represents an external force, which in our problem is gravity. The boundary conditions between the fluid and the oblate ellipsoid particles are satisfied considering that the fluid motion on the particle surface is subject to the non-slip boundary condition:

$$\vec{v}(\vec{x}) = \vec{v_t} + \vec{r}(\vec{x})_{CM} \times \vec{\omega} \tag{2}$$

where $\vec{v_t}$ is the translational velocity of the ellipsoid, $\vec{r}(\vec{x}_{CM})$ the vector from its center to the point $\vec{x}$ at the ellipsoid surface, and $\vec{\omega}$ the ellipsoid angular velocity. The interaction between the ellipsoidal surface and the fluid adjacent
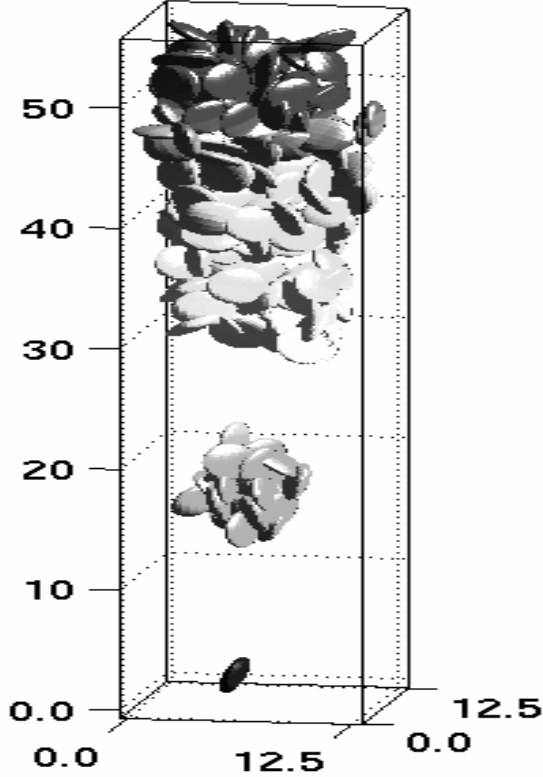
Fig. 1. Snapshot of the oblate ellipsoids falling in a fluid. The picture shows the "cluster" formation. The ellipsoid aspect-ratio is $\Delta r = 0.4/1.5$, the distance is given in units of the larger radius R_M, the Reynolds number is $Re = 4 * 10^{-2}$ and the particle volume fraction is $\Phi_V = 0.05$.

to the ellipsoid is achieved by setting a restoring force that gives rise to a "distribution force" in the body term of the Navier Stokes equation. This distribution force mimics the presence of the ellipsoids in the sense that the fluid inside the ellipsoid moves like a rigid body. A restoring force is applied whenever the template particle and the fluid rigid body are not in the same position [11].

The repulsive force between the ellipsoids is chosen proportional to their overlap. When the oblate ellipsoids are non-overlapping the force is zero and at short distances the hydrodynamic forces describing the existence of the fluid avoid the contact between the particles [12]. For this force, we choose a contact function explained in depth in [12] and [13] . The geometry of the oblate ellipsoid is characterized by Δr, its aspect-ratio is defined as the ratio of the minimum radius R_m to the maximum radius, R_M:

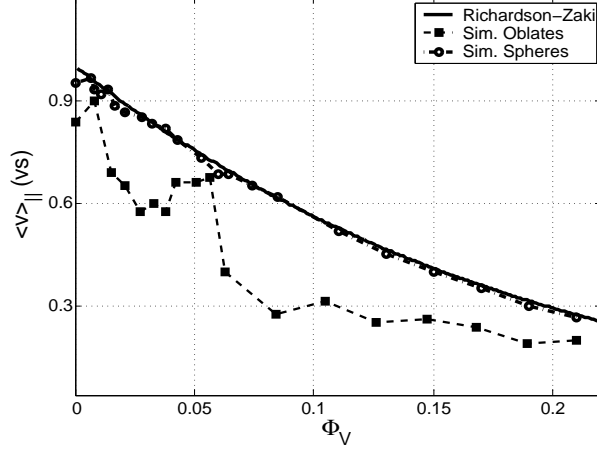$$\Delta r = \frac{R_m}{R_M} \tag{3}$$

Fig. 2. Mean sedimentation velocity $v(t)_\parallel$ for the oblate ellipsoid (dash-squared line) and sphere (dash-dot line), as function of the volume fraction Φ_V. The oblate ellipsoid aspect-ratio is $\Delta r = 0.4/1.5$, the radius of the equivalent sphere $R_{equi} = 0.97$ and the Reynolds number $Re = 4 * 10^{-2}$.

We define the equivalence between the sphere and an oblate ellipsoid as the sphere that has the same volume, with the equivalent radius:

$$R_{equi} = \sqrt[3]{R_m R_M^2} \tag{4}$$

The Reynolds number is defined as:

$$Re := \frac{2 R_M v_s \rho_f}{\nu} \tag{5}$$

where v_s is the mean vertical oblate ellipsoid velocity, $2 * R_M$ being the characteristic length, ρ_f is the density and ν is the dynamical viscosity of the fluid. The number of ellipsoids in our simulations is of the order of one thousand. We choose the density of the fluid, the Stokes velocity and the larger radius of the ellipsoid equal to unity in our system. In all cases the container has a height, $L = 85$ and a base of 12.5×12.5, and the lattice constant, $h = 0.7$. The ratio between the density of the oblate ellipsoids and the fluid is 4.

3 Results

3.1 Sedimentation velocity for oblate ellipsoids

In fig. 2 we show the mean vertical sedimentation velocity $v(t)_\parallel$ as a function of the volume fraction Φ_V, within a range of 0.01 to 0.21, for oblate ellipsoids
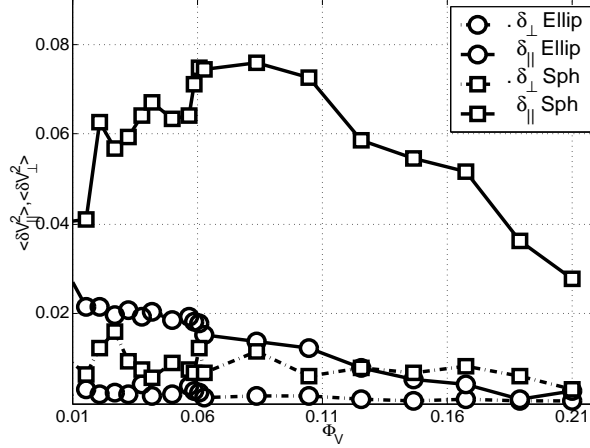
Fig. 3. Velocity fluctuations for ellipsoids (circle-line) and spheres (squared-line) for the vertical (solid line), and horizontal (dash-dot line) components corresponding to fig. 1. The oblate ellipsoid has an aspect-ratio of $\Delta r = 0.4/1.5$, the equivalent radius of a sphere is $R_{equi} = 0.97$, and the Reynolds number $Re = 4 * 10^{-2}$.

and spheres and then compared to the phenomenological Richardson-Zaki law $\frac{V(\Phi)}{V_0} = (1 - \Phi_V)^n$ [3] with $n = 5.5$. The limit of $\Phi_V \to 0$ corresponds to the single falling ellipsoid which we studied in our previous work [15]. It is interesting to point out that the sedimentation velocity of the ellipsoid, is small compared to that of the sphere, which follows the phenomenological Richardson-Zaki law. This is not the case for fibers (elongated ellipsoids), where it is found that the sedimentation velocity has a maximum for smaller volume fraction which can exceed the terminal velocity of a single fiber [14].

For oblate ellipsoids the mean vertical sedimentation velocity passes through a local maximum at $\Phi_V \approx 0.05$. This maximum is quite interesting since it is not observed for spheres. Similar non-monotonic sedimentation of non-spherical bodies (e. g. fibers) has been reported experimentally by Herzhaft et. al.[9] and for prolate ellipsoids in simulations by Kuusela et al. [12] due to an orientation parallel to gravity.

In fig. 3 we present the parallel ($\parallel$) and perpendicular ($\perp$) components of the velocity fluctuations with respect to gravity as a function of the volume fraction Φ_V which are defined as:

$$\delta V_{\parallel}^2 = <V_{\parallel}^2> - <V_{\parallel}>^2 \tag{6}$$

$$\delta V_{\perp}^2 = <V_{\perp}^2> \tag{7}$$

The angular brackets indicate averaging over the ellipsoids that have not reached the final bottom position at the container. The averages were made over at least 50 realizations starting with different random postions and orientations. In fig. 3 the vertical (parallel to gravity) fluctuations for spheres and
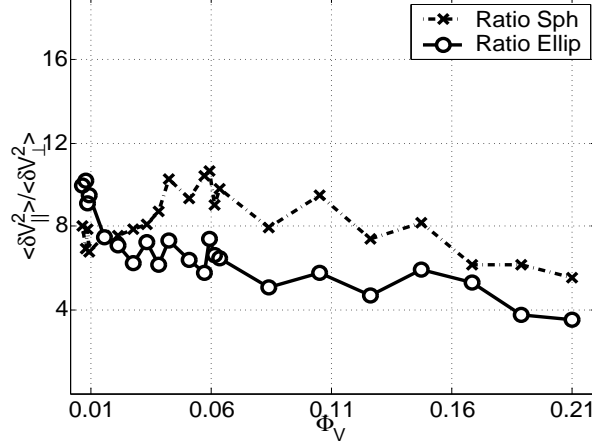
5

Fig. 4. Ratio of the vertical to the horizontal velocity fluctuations for spheres and oblate ellipsoids as function of the volume fraction, Φ_V. The oblate ellipsoid aspect-ratio is $\Delta r = 0.4/1.5$, and the Reynolds number $Re = 4*10^{-2}$.

for ellipsoids are much larger than the respective horizontal components. The fluctuations for ellipsoids decrease with the volume fraction. For an equivalent system of spheres, the fluctuations show a maximum at intermediate volume fractions ($\Phi_V \approx 0.07$) [16,17]. In all cases the fluctuations for the spheres are considerably larger than the fluctuations for oblate ellipsoids.

In fig. 4 we present the ratio, $\delta V_{||}^2/\delta V_{\perp}^2$ for spheres and oblate ellipsoids. For spheres the ratio shows a maximum around $\Phi_V \approx 0.07$ [16,17]. For ellipsoids the ratio shows a slightly larger value than that of the spheres for very small volume fractions and has an overall monotonic decrease with the volume fraction.

We display the ratio of the vertical velocity fluctuations for spheres to that of the ellipsoids in fig. 5. The quotient exhibits a linear behavior with the volume fraction following approximately the relation $(\delta V_{vert,sph}^2/\delta V_{vert,ellip}^2) = 88 * \Phi_V + 0.76$. The inset shows the horizontal case, also a linear behavior $(\delta V_{hor,sph}^2/\delta V_{hor,ellip}^2) = 33 * \Phi_V + 3$.

In figure 6 we present the parallel, $\tau_{||}$ and perpendicular, $\tau_{\perp}$ components of the autocorrelation time for both ellipsoids and spheres. We use the definition of the correlation time as:

$$\tau_c = \frac{1}{C(0)} \int_0^{\infty} C(t)dt \tag{8}$$

Where $C(t)$ is the particle velocity autocorrelation function which is defined as $C(t) = <\delta V(t)\delta V(0)>$. Here $\delta V(t) = V(t) - <V>$ is the local velocity fluctuation, where $<V>$ was taken as the mean (horizontal or vertical) velocity.
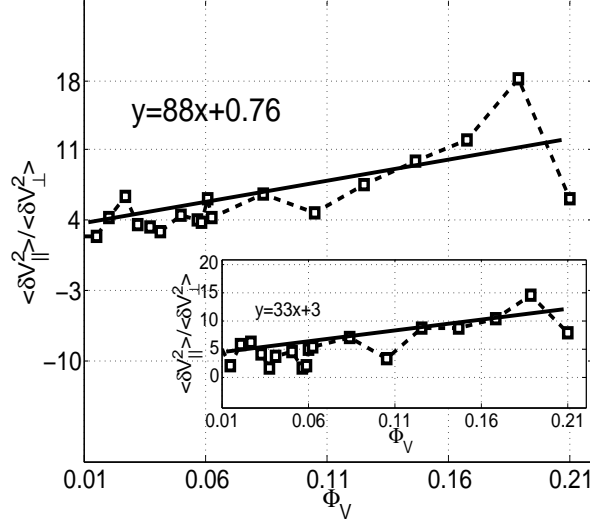
6

Fig. 5. Ratio of the vertical velocity fluctuations for spheres to that of the oblate ellipsoids as function of the volume fraction, Φ_V. The inset shows the corresponding ratio for the horizontal fluctuations. The oblate ellipsoid aspect-ratio is $\Delta r = 0.4/1.5$, and the Reynolds number $Re = 4 * 10^{-2}$.
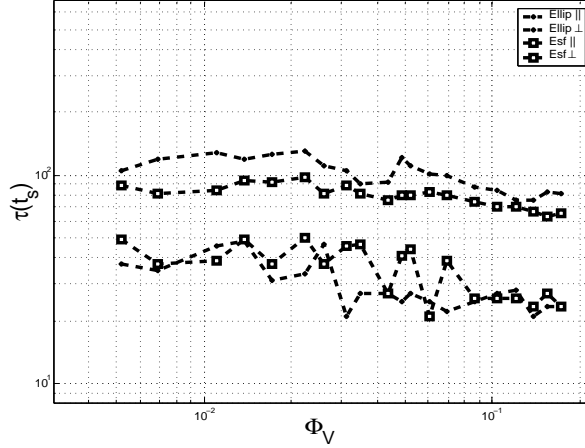

Fig. 6. Autocorrelation times τ (in units of t_s) as function of the volume fraction Φ_V for oblate ellipsoids and the equivalent spheres split into components parallel ($\parallel$) and perpendicular ($\perp$) to gravity. The oblate ellipsoid aspect-ratio is $\Delta r = 0.4/1.5$, the equivalent sphere system has a radius $R_{equi} = 0.97$ and the $Re = 4 * 10^{-2}$. The results are plotted in a log-log scale.

The vertical component, shows an overall large value for the oblate ellipsoids compared to that of the spheres. The horizontal components of the autocorrelation time between oblate ellipsoids and spheres are indistiguishable.

In figure 6 the four curves decay as power laws given by $\tau \approx \Phi^{-\alpha}$, We see that the values of α for the parallel and perpendicular components for ellipsoids are $\alpha_\parallel \approx 0.11$ and $\alpha_\perp \approx 0.16$ respectively and that for the spheres are $\alpha_\parallel \approx -0.10$ and $\alpha_\perp \approx 0.22$ respectively
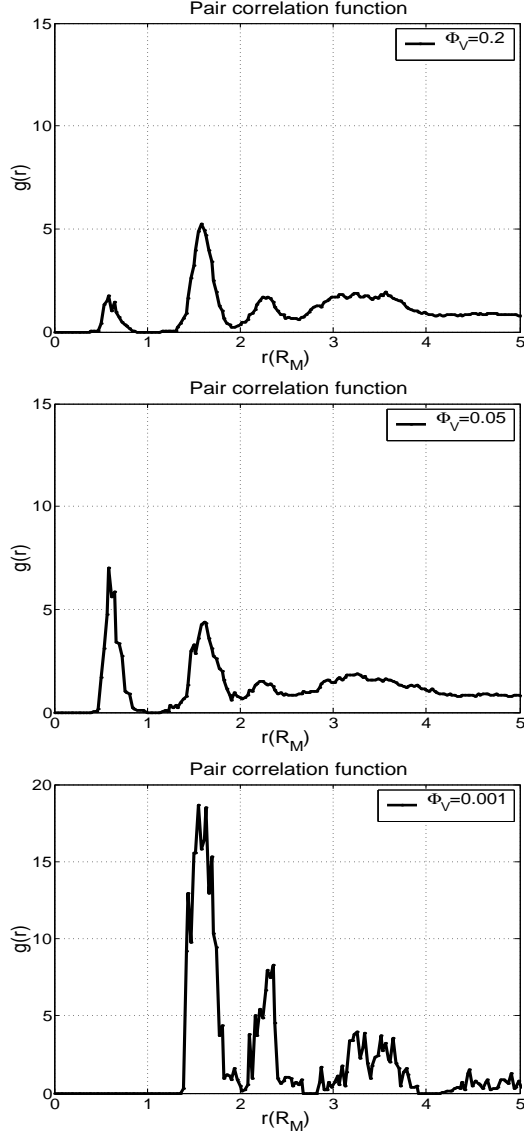
Fig. 7. Pair distribution functions for oblate ellipsoids for different volume fractions, Φ_V. The Reynolds number $Re = 4*10^{-2}$.

We calculate the pair correlation function for different volume fractions Φ_V and the results are shown in fig. 7. The pair correlation function, for smaller volume fractions $\Phi_V = 0.001$, clearly shows large inhomogeneities in the sense that there is a "packing formation" as seen in fig. 1, of oblate ellipsoids. These inhomogeneities disappear for large volume fraction $\Phi_V \geq 0, 2$. Furthermore, in the intermediate case for $\Phi_V = 0.05$ we can see in the pair correlation function that the first peak is close to the origin, located at $r = 0.6$, which is also present at $\Phi_V = 0.2$ but smaller. This additional larger peak at $\Phi_V = 0.05$ could be related to the local maximum in the sedimentation velocity fig. 2. By looking at the snapshots as the one shown in fig. 1 one sees that entire bundles of aligned particles seem to detach and move down faster which might well be the origin of this peak. This kind of "bundle behavior" has also been observed
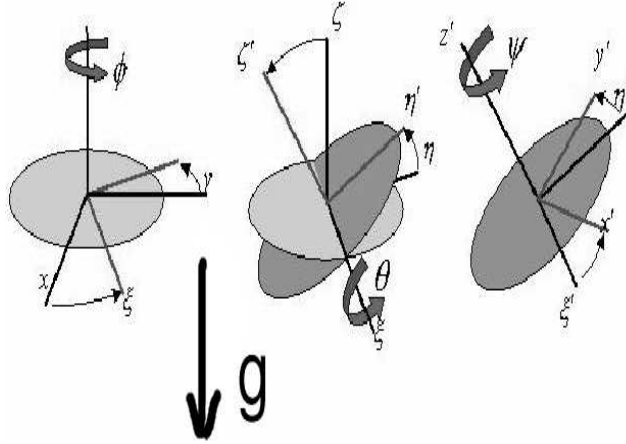
8

Fig. 8. Euler angles ϕ, θ and ψ used for the description of the oblate ellipsoid orientational behavior [17].

in the sedimentation of fibers ref [9] where these bundles settle faster than the individual fibers.

3.2 Orientational behavior

For the measurement of the orientation we use the Euler angles described in fig. 8. The mean vertical orientation (MVO), θ , as a function of the volume fraction, is shown in fig. 9. For smaller volume fraction the MVO shows more alignment with gravity and in the limit $\Phi_V \to 0$ a closer alignment with gravity is observed which corresponds to the orientational behavior for one oblate ellipsoid observed in [15]. We also see for the MVO an intermediate maximum, at $\Phi_V \approx 0.05$, which could explain the local vertical velocity maximum at the same volume fraction shown in fig. 2. This intermediate maximum is not present for spheres. For larger values of the volume fraction, $\Phi_V > 0.08$ the plot shows a monotonic decrease.

Figure 10 shows the orientational distribution function $P(cos(\theta))$ for the vertical angle, θ, for different volume fractions, Φ_V. For smaller volume fractions, $\Phi_V = 0.008$ the orientational distribution shows a maximum around $cos(\theta) \approx 0.1$ in agreement with fig. 9. The limiting case ($\Phi_V \to 0$), i.e., one sedimenting oblate ellipsoid, studied by us in [15], presents a vertical alignment with gravity ($\theta \approx 90^o$), and in fig 9 we can see a value of $\theta \approx 85^o$.

As the volume fraction increases, the distributions flatten, and at $\Phi_V = 0.05$ the distribution shows a moderate maximum around $cos(\theta) \approx 0.45$, corresponding to the similar intermediate maximum in figures 9 and 2. We conclude that the vertical velocity is influenced significatively by the orientational behavior along gravity, as it is well known for other spheroid systems [8].
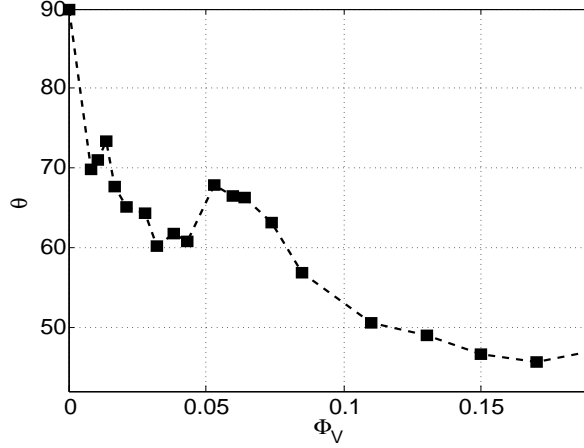
9

Fig. 9. Mean vertical orientation θ for oblate ellipsoids as a function of the volume fraction Φ_V. The oblate ellipsoid aspect-ratio is $\Delta r = 0.4/1.5$, and the Reynolds number $Re = 4 * 10^{-2}$.
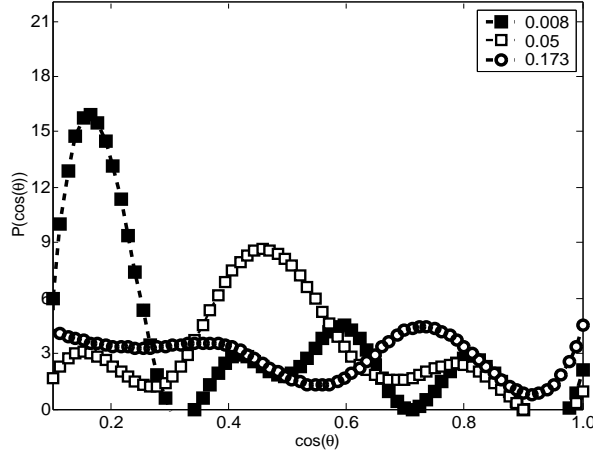

Fig. 10. The distribution function $P(cos(\theta))$ for the mean vertical orientation θ for different volume fractions. The ellipsoid aspect-ratio is $\Delta r = 0.4/1.5$, and the Reynolds number $Re = 4 * 10^{-2}$.

Figure 11 shows the orientational distribution function $P(cos(\phi))$ for the angle ϕ, for different volume fractions, Φ_V. The orientation around the vertical slightly increases for smaller volume fractions, and decreases with larger volume fractions. Similar behavior is also found for the third Euler angle ψ. We conclude that the Euler angles ϕ and ψ are not much influenced by the volume fraction.

3.3 Orientational changes

To quantify the orientation of the oblate ellipsoids we introduce the quantity $\Psi =< 2cos(\theta) - 1 >$ that was also used in [8], [9] as orientational order
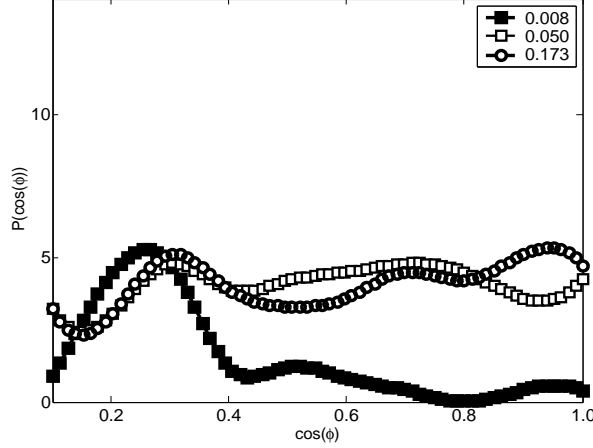
Fig. 11. The distribution function $P(cos(\phi))$ for the mean vertical orientation ϕ for oblate ellipsoids. The aspect-ratio is $\Delta r = 0.4/1.5$, and the Reynolds number $Re = 4 * 10^{-2}$.

parameter, it would give -1, 0 or $+1$ if all the oblate ellipsoids were perpendicular to gravity, randomly oriented or aligned with gravity respectively. Figure 12 shows the behavior of Ψ against Φ_V, for smaller volume fractions, $\Phi_V \approx 0.001 - 0.08$ the order parameter takes negative values evidencing the alignment along gravity and in agreement with the limit, $\Phi_V \rightarrow 0$ (one oblate ellipsoid) [15]. Approximately at $\Phi_V \approx 0.08$ the order parameter is zero. For larger $\Phi_V \geq 0.08$ a positive order parameter implies the orientation is perpendicular to gravity.

In the range of $\Phi_V \approx 0.001 - 0.08$, Ψ has a local minimum close to $\Phi_V \approx 0.05$ where we found a local maximum in fig. 9 and fig. 2. The simulations were repeated with two other different aspects ratios $A_r = 0.4/0.8; 0.4/2.4$ and we observed similar behavior. In the case of one oblate ellipsoid ($\Phi_V \rightarrow 0$) the order parameter Ψ has a value very close to -1 as the ellipsoid aspect-ratio is increased [15].

3.4 Moderate Reynolds number

Figure 13 presents the mean vertical sedimentation velocity for oblate ellipsoids ($\square$ squared line) and the equivalent spheres ($\circ$ circle lined) as a function of the volume fraction at moderate Reynolds number ($Re \approx 7$). In our previous work this simulation method has been used with success up to $Re \approx 10$ [11] and [14]. The intermediate maximum for the ellipsoids is not observed in fig. 13 as seen in fig. 2 at low Reynolds number.

A comparison with the phenomenological Richardson-Zaki law (continous line in fig 13) shows an exponent around $n_{Sph} = 3.2$ for spheres and $n_{Ellip} = 4.0$ for ellipsoids. In both both cases, the data follow the Richardson-Zaki law
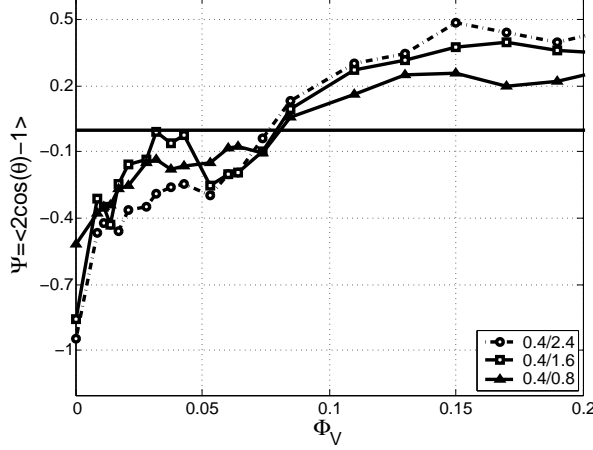
Fig. 12. Order parameter Ψ as a function of the volume fraction, Φ_V for three different aspect-ratios $\Delta r = 0.4/2.4$; $0.4/1.6$; $0.4/0.8$.
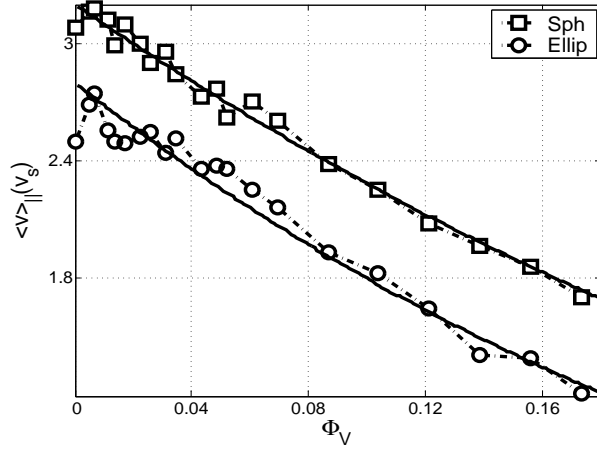

Fig. 13. Mean sedimentation velocity $v(t)_\parallel$ for the oblate ellipsoid (dash-squared line) and a sphere (dash-circle line), as function of the volume fraction, Φ_V. The oblate ellipsoid aspect-ratio is $\Delta r = 0.4/1.5$, the equivalent sphere has $R_{equi} = 0.97$ and the Reynolds number $Re \approx 7$.

rather closely. These exponents ($n_{Sph} = 3.2$ and $n_{Ellip} = 4.0$) are between the low particle Reynolds number limit ($n \approx 4.5$) and a turbulent particle system ($n \approx 2.5$), [3].

Figure 14 (top) presents the vertical distribution function, $P(\cos(\theta))$ at moderate Reynolds number. For all volume fractions, $P(\cos(\theta))$ presents a larger distribution around $cos(\theta) \approx 0$ ($\theta \approx 90^o$), which tends to be much flatter ($cos(\theta) \geq 0.15$) than in fig. 10. For the other angular variables, ϕ and ψ, the distributions show a peak around $\cos(\phi) \approx 0$, $\cos(\psi) \approx 0$, and for larger volume fractions, they follow a constant behavior.

The bottom of fig. 14 shows the behavior of the orientational parameter Ψ at moderate Reynolds number. For one oblate ellipsoid ($\Phi_V \to 0$), the value of
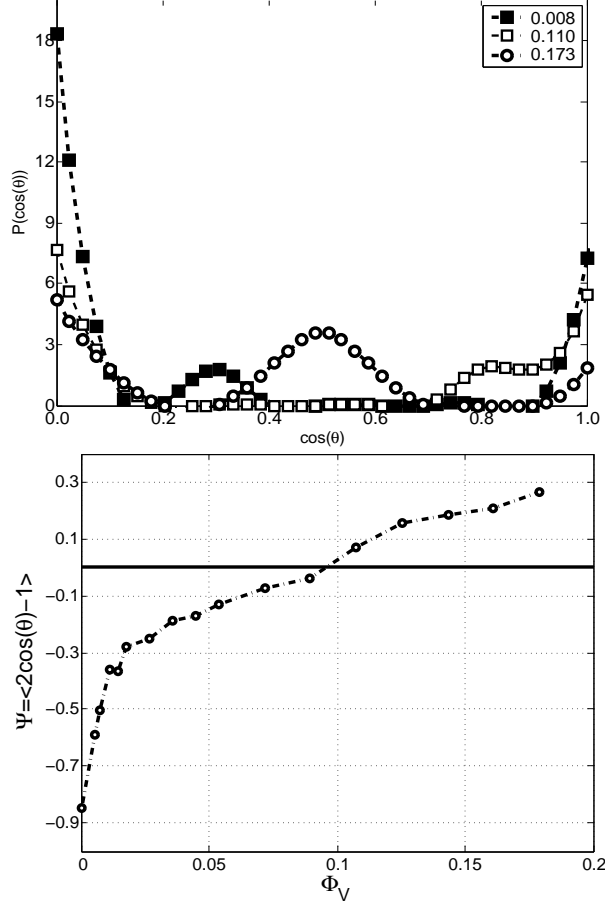
12

Fig. 14. The top picture shows the distribution function, $P(cos(\theta))$ of the mean vertical orientation at different volume fraction Φ_V. The bottom picture shows how the order parameter behaves with the volume fraction Φ_V. The oblate ellipsoid aspect-ratio is $\Delta r = 0.4/1.5$, the equivalent sphere has $R_{equi} = 0.97$ and the Reynolds number $Re \approx 7$.

Ψ is closer to -1 (vertical alignment), as in the case of low Reynolds number fig. 11. The intermediate maximum is not seen in figure 12, and the point at which the orientational parameter Ψ vanishes, is shifted slightly to the right ($\Phi_V \approx 0.1$) fig. 14 (bottom). This shift in Ψ is also seen in the case of fibers, when the Reynolds number increases, by a factor of 5, [14].

4   Outlook and Conclusions

We have simulated the sedimentation of oblate ellipsoids at small volume fraction ($\Phi_V \leq 0.2$) and small Reynolds number ($Re \approx 10^{-2}$). We have found that at intermediate volume fraction the settling velocity exhibits a local maximum which to our knowledge has never been reported in the literature. It would be desirable to experimentally verify this maximum.

This local maximum in the velocity can be related to the non monotonic behavior of the vertical orientation of the oblate ellipsoids along gravity, which is shown in figures 9, and 10, and can be explained by the "cluster" formation shown in fig. 1, which is also found in fiber-like suspensions [9].

At low Reynolds number the orientational order parameter Ψ vanishes around $\Phi_V \approx 0.08$ fig. 9. As Φ_V decreases the orientational alignment with gravity increases as shown in fig. 9 and 14 (bottom), as for low and moderate Reynolds number and in the limit $\Phi_V \to 0$ a single ellipsoid aligns with gravity, which is a distinctive feature of the steady-state regime for a single oblate ellipsoid as reported in references [15] and [19].

We also present data at moderate Reynolds number ($Re \approx 7$) for the sedimentation velocity of oblate ellipsoids as the volume fraction Φ_V is increased. As in the case of low Reynolds number the ellipsoids have a smaller sedimentation velocity than the equivalent spheres, fig. 2 and 13. The data for ellipsoids and spheres follow the Richardson-Zaki law [3] with exponents ($n_{Ellip} \approx 3.2, Re = 10^{-2}$) and ($n_{Sph} \approx 4.0, Re = 7$) respectively. The $P(\cos(\theta))$ distribution presents a larger alignment of ellipsoids with gravity compared to those with small Reynolds number. The vanishing of the order parameter is slightly shifted ($\Phi_V \approx 0.1$) to the right as the Reynolds number increases (see fig 14, bottom). The alignment with gravity is present for small and moderate Reynolds number as $\Phi_V \to 0$, as shown in fig. 14 (top) and fig. 10, which is in agreement with the orientational behavior of a single ellipsoid [15]. All the simulations in this work are located in the steady-falling regime of our previous work [15] for a single oblate ellipsoid.

One open problem that should be addressed in the future is the behaviour of velocity fluctuations as the container system size and the ellipsoid aspect-ratio increases. This work has been carried out for sedimenting spheres but not for ellipsoids, [1].

5   Acknowledgments

References

[1] S. Ramaswamy *Adv. in Phys.* **50**, 297-341 (2001)

[2] G. K. Batchelor *J. Fluid Mech.* **52**, 245-268 (1972).

[3] J. F. Richardson and W. N. Zaki *Trans. Inst. Chem. Engr.* **32**, 35 (1954).

[4] G. K. Batchelor *J. Fluid Mech.* **44**, 419-440 (1970).

[5] P. Olla, *Phys. Rev. Lett.* **82**, 453 (1999).

[6] Q. Dewei, L. Luo, R. Arawamuthan and W. Strieder. *J. Stat. Phys.* **107**, 101 (2002).

[7] http://www.pulpandpapercanada.com.

[8] E. Kuusela, J. M. Lahtinen, and T. Ala-Nissila *Phys. Rev. Lett.* **90**, 094502 (2003).

[9] B. Herzhaft and E. Guazzelli. *J. Fluid Mech.* **384**,133 (1999).

[10] K. Höefler .*Simulation and Modeling of Mono- and Bidisperse Suspensions. Doctoral Thesis.Stuttgart University.* (2000).

[11] K. Höefler and S. Schwarzer, *Phys. Rev. E* **61**,7146 (2000).

[12] E. Kuusela, K. Höefler, and S. Schwarzer *J. of Engineering Mathematics* **41**,221 (2001).

[13] J. W. Perram, J. Rasmussen, E. Praestgaard and J. L. Lebowitz. *Phys. Rev. E.* **54** 6565 (1996).

[14] E. Kuusela, J. M. Lahtinen, and T. Ala-Nissila *Phys. Rev. Lett.* **90**, 094502 (2003).

[15] F. Fonseca, H. Herrmann, submitted to *Phys. Rev. E.* (2003)

[16] W. Kalthoff, S. Schwarzer, G. Ristow, and H. Herrmann. *Int. J. Mod. Phys. C* **7(4)** 543 (1996).

[17] H. Nicolai, B. Herzhaft, E: J. Hinch, L. Oger and E. Guazzelli *Phys. Fluids* **7(1)** 12 (1995).

[18] H. Goldstein, C. Poole and D. J. Safko. Classical Mechanics. *Addison Wesley, San Francisco, 2002*

[19] G. P. Galdi, M. Pokorny, A. Vaidya, D.D. Joseph and J. Feng. *J. Math. Fluid Mech.* **3**, 183 (2001).